Enhanced production of reactive oxygen species in HeLa cells under concurrent low-dose carboplatin and Photofrin® photodynamic therapy

YOUNSHICK CHOI[1], JI-EUN CHANG[2], SANGHOON JHEON[2], SEI-JUN HAN[3] and JONG-KI KIM[1]

[1]Departments of Biomedical Engineering and Radiology, School of Medicine, Catholic University of Daegu, Daegu 42472; [2]Department of Thoracic Surgery, Seoul National University Bundang Hospital, Seongnam, Gyeonggi 13620; [3]Department of Obstetrics and Gynecology, Chosun University School of Medicine, Gwangju 501759, Republic of Korea

Received November 3, 2017; Accepted April 13, 2018

DOI: 10.3892/or.2018.6415

Abstract. Concurrent low-dose carboplatin/Photofrin® photodynamic therapy (ccPDT) has been shown to promote relapse-free complete tumor regression in cervical or endometrial cancer patients as a fertility-preservation therapy. This study aimed to investigate the molecular mechanism of the enhanced therapeutic efficacy of ccPDT by determining intracellular reactive oxygen species (ROS) and necrotic or apoptotic cell damage in HeLa cells loaded with fluorescent oxidant agents and Photofrin or/and carboplatin under light irradiation. The cytotoxic effects of ccPDT were compared when monitored with a light dose under carboplatin or Photofrin alone. Photofrin-PDT alone did not enhance either hydroxyl radicals ($OH^{\bullet}$) or superoxide anions ($O_2^{\bullet -}$), but a slight enhancement of hydrogen peroxide (H_2O_2) production was observed. A larger enhancement of ROS production was obtained in a dose-dependent manner following ccPDT, especially $OH^{\bullet}$ and H_2O_2, in conjunction with both necrotic and apoptotic cell death, compared with necrotic-prone PDT alone. The carboplatin-mediated Fenton reaction: $2[Pt^{II}]_2 + H_2O_2 \rightarrow [Pt^{2.25}]_4 + OH^- + OH^{\bullet}$ was proposed to explain the dose-dependent enhancement of $OH^{\bullet}$. In conclusion, the therapeutic enhancement of ccPDT *in vitro* was attributable to the carboplatin-mediated synergetic production of $OH^{\bullet}$ and apoptotic cellular damage, compared with Photofrin-PDT alone.

Introduction

Photodynamic therapy (PDT) is a local therapy; thus, in principle, PDT can be safely combined with any systemic therapy by exploiting non-overlapping cellular targets. Previous studies have demonstrated the enhancement of the therapeutic efficacy of combination treatment with carboplatin (CBP) and PDT (1-7) through synergism (2) and the subsequent ROS-mediated downregulation of biological functions (3,4) or modulation of EGRF/PARP protein expression (5). In particular, low-dose CBP combined with Photofrin®-PDT (ccPDT) resulted in a relapse-free period of more than 3 years when used to treat cervical or endometrial cancer patients, while also preserving fertility and enabling the successful delivery of babies, as determined in our previous clinical efficacy study (1). However, the involvement of specific reactive oxygen species (ROS) and related cell death pathways in the therapeutic enhancement by ccPDT remains to be elucidated despite ROS-mediated synergistic therapeutic enhancement becoming increasingly evident (2-4). Anticancer metal complexes (platinum, gold, arsenic, ruthenium, rhodium, copper, vanadium, cobalt, manganese, gadolinium and molybdenum) have been shown to strongly interact with or even disturb cellular redox homeostasis, and ROS generation via the Fenton reaction is known (8).

The destructive power of large-scale ROS production is highlighted by the fact that PDT uses photoactivation of chemicals that produce ROS; primarily, but not exclusively, singlet oxygen ($^1O_2$), to kill cancer cells and to treat local infections (9). The predominant type of ROS generated by the photosensitizer depends on the type of assembly of photosensitizer molecules (monomer, dimer), the reaction and local oxygen concentrations, such that Type I reactions produce $O_2^{\bullet -}$ while type II produce $^1O_2$ (10,11). It was suggested that $^1O_2$ produced at plasma/ER/Golgi membranes mediates necrosis, whereas ROS other than $^1O_2$ likely produced by the mitochondria, activate the intrinsic apoptosis pathway (4,9,11-13). While most clinically approved photosensitizers (porphyrins, chlorins, or chemically related species) have high efficiency to produce $^1O_2$ (9,11), enhanced ROS production via either electron or energy transfer or a new cytotoxic pathway may improve the therapeutic efficacy of combined treatment with different biological consequences compared to PDT alone. In this study, ccPDT-induced modulation of ROS production and cellular death were examined to elucidate the mechanism of the therapeutic efficacy in ccPDT.

Correspondence to: Professor Jong-Ki Kim, Departments of Biomedical Engineering and Radiology, School of Medicine, Catholic University of Daegu, Daegu 42472, Republic of Korea
E-mail: jkkim@cu.ac.kr

Key words: concurrent carboplatin/Photofrin® PDT, ROS, Fenton reaction, apoptosis, redox active platinum

Materials and methods

Materials. Photofrin® was kindly provided by LightpharmTech (Seoul, Korea). Carboplatin was purchased from Sigma-Aldrich (Merck KGaA, Darmstadt, Germany). Fetal bovine serum (FBS) was purchased from MP Biomedicals, LLC (Solon, OH, USA). RPMI-1640, PBS and penicillin-streptomycin (P/S) were obtained from Gibco BRL (Thermo Fisher Scientific, Inc., Waltham, MA, USA). Aminophenyl fluorescein (APF), dihydroethidium (hydroethidine, DHE), and H_2DCFDA were obtained from Molecular Probes (Thermo Fisher Scientific, Inc., Waltham, MA, USA). ROSstar™ 650 was purchased from LI-COR Biosciences (Lincoln, NE, USA). The Apoptosis/Necrosis Detection Kit (blue, red, green; ab176750) was obtained from Abcam (Cambridge, UK). The HeLa cell line was purchased from the Cell Bank of the Committee of Type Culture Collection (Seoul, Korea). The 96-well plates (clear/black) and 4-well cell culture slides were supplied by SPL Life Sciences (Pocheon, Korea).

Carboplatin cytotoxicity test to determine the non-toxic dose. To establish the low-dose response rate of HeLa cells to carboplatin (CBP), cells were treated with 0-1,000 μM CBP in standard media. HeLa cells were cultured at 37˚C in a 5% CO_2 humidified atmosphere in RPMI-1640 medium supplemented with 10% (v/v) fetal bovine serum (FBS) and 1% (v/v) P/S. Four batches of cells for each CBP concentration were prepared by seeding at a density of $1x10^5$ cells/ml onto clear 96-well plates and incubated overnight. After changing to a medium containing 0, 5, 20, 100 and 1,000 μM CBP, the cells were incubated in the dark for 24 h, and the cytotoxicity was measured using the MTT (3(4,5-dimethylthiazol-2-yl)-2,5-diphenyltetrazolium bromide) assay.

Concurrent Photofrin and CBP treatment. HeLa cells at a density of $1x10^5$ cells/ml were seeded in 96-well plates (clear/black) or 4-well cell culture slides, and incubated overnight. After washing with PBS twice, the cells were incubated with 20 μM Photofrin-containing medium for 3 h, or/and washed twice with PBS, and re-incubation with 100 μM CBP-containing medium. Medium was replaced with PBS prior to light irradiation.

Assessment of ROS levels. Five wells of cells per group were seeded and treated as described above with concurrent Photofrin and CBP treatment in 44 black 96-well plates. After twice washing, 4 ROS probe groups of each 11 plates were incubated with medium containing 1 μM of APF, 5 μM of DHE, 25 μM of ROSstar™ 650, and 1 μM of H_2DCFDA in the dark separately for 30 min. The cells were then washed twice and placed in PBS, and light irradiation was performed using a 630-nm laser with an intensity of 2.5 mW/cm^2 for 0, 100, 200, 300, 400, 500, 600, 700, 800, 900 and 1,000 sec. The generation of each type of ROS was measured by fluorescence intensity using a plate reader set at the appropriate wavelength: APF, λ_{ex}=465 nm/λ_{em}=510 nm; DHE, λ_{ex}=510 nm/λ_{em}=590 nm; ROSstar™, λ_{ex}=635 nm/λ_{em}=670 nm, and H_2DCFDA, λ_{ex}=510 nm/λ_{em}=535 nm.

Apoptosis/necrosis assay. Cells prepared in 4-well cell culture slides were treated according to the above concurrent Photofrin and CBP treatment. Cells were treated by light irradiation at: λ=630 nm; fluence rate, 2.5 mW/cm^2; light dose, 660 mJ. After treatment, the medium was replaced, and cells were incubated for 24 h. The apoptosis/necrosis assay was performed according to the manufacturer's instructions. Cells were treated with a mixture of staining solutions: 20 μl of Apopxin™ Deep Red Indicator (100X) for apoptotic cells, 10 μl of Nuclear Green DCS1 (200X) for necrotic cells, 10 μl of CytoCalcein Violet 450 (200X) for viable cells, and 2 ml of assay buffer. The cells were then incubated for 30 min at room temperature, washed two times with assay buffer, and finally analyzed by confocal microscopy with the following wavelengths: Apopxin Deep Red Indicator; λ_{ex}=640 nm/λ_{em}=663-738 nm; Nuclear Green DCS1, λ_{ex}=488 nm/λ_{em}=500-550 nm; and CytoCalcein violet 450, λ_{ex}=405 nm/λ_{em}=425-475 nm.

Cell viability assay. Each group contained 4 (wells) x11 slide samples for multiple irradiation doses. HeLa cells were prepared for each experimental group by seeding at a density of $1x10^5$ cells/ml in 96-well plates (clear/black) or 4-well chamber cell culture slides, and incubated overnight. After washing twice with PBS, the cells were incubated with 20 μM Photofrin-containing medium for 3 h, washed twice with PBS and re-incubated in 100 μM CBP-containing medium. Four different experimental groups were prepared; cells incubated with no drugs (control), Photofrin (PF), carboplatin (CBP), or Photofrin and carboplatin (PF+CBP; ccPDT). The medium was replaced with PBS prior to light irradiation. Light irradiation was performed with a fluence rate of 2.5 mW/cm^2 at various light doses: 0, 330, 660, 990, 1,320, 1,650, 1,980, 2,310, 2,640, 2,970, 3,300 mJ for which the total area irradiated was 1.32 cm^2. Cell viability was determined using the MTT assay 4 h after light irradiation.

Statistical analysis. ROS-fluorescence intensity and OD_{540} data on the viability levels are presented as the mean ± standard deviation (SD). One-way analysis of variance (ANOVA) was used for data analyses. The Levene's test was used to demonstrate the equal variances of the variables. Post hoc analysis using Bonferroni's multiple comparison was used to determine significant differences. All testing was performed using IBM SPSS statistical software v23 (IBM Corp., Armonk, NY, USA).

Results

Cytotoxicity of carboplatin- and PF-mediated PDT. Significant CBP-mediated cytotoxicity was not induced in HeLa cells treated with up to 100 μM CBP, as shown in Fig. 1. When treated with 1 mM of CBP, cell viability was decreased by 30%. Thereafter, 100 μM CBP was used in further ROS measurement studies or cytotoxicity assays for the combined treatment.

When the cells were treated with 100 μM CBP in combination with varying light doses and 20 μM Photofrin (PF+CBP), the percentage of cell viability was decreased significantly ($P<0.001$) compared to each individual treatment alone (Fig. 2). When treated with 330 mJ of light, Photofrin (PF)-PDT did not produce significant cytotoxicity, while ccPDT (PF+CBP) treatment showed a 50.2±25.4 or 42.8±28.2% reduction in viable cells compared to the control or PF-PDT alone,

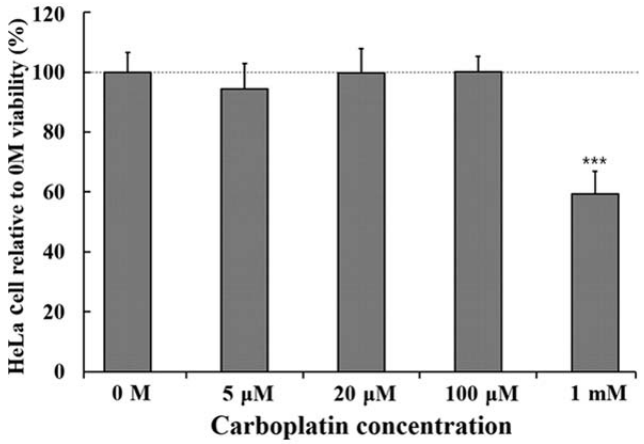

Figure 1. Cytotoxicity of HeLa cells treated with increasing concentrations of carboplatin (0-1,000 μM). Cytotoxicity was determined by MTT assay. Data represent the mean ± SD (n=4 per group). ***P<0.001 compared with 0 M.

respectively. The enhanced reduction in cell viability reached 67.5±6.9 or 43.7±3.1% compared to the control or PF-PDT alone, respectively, when treated with the light dose of 660 mJ. The relative cytotoxicity ratio of combined treatment to PF-PDT alone gradually increased from 1.74 to 3.54 with a light dose ranging from 330 to 3,300 mJ.

Increased apoptotic effect following combined treatment. Triple staining with Apopxin Deep Red Indicator, Nuclear Green DCS1, and CytoCalcein Violet 450 was performed to determine the cellular damage pathway for individual and combined treatments. As shown in Fig. 3, the dominate pathway for PF-PDT alone was necrotic death, while enhanced apoptosis was observed for ccPDT. Light irradiation in the presence of CBP or PF alone demonstrated slight apoptosis, 6.0±2.1 or 3.3±1.8% in average for multiple sample batches, respectively, based on counting cells in fluorescence images, but this apoptotic effect increased notably (35.2±9.4%) following PDT treatment under the coexistence of CBP and Photofrin (ccPDT).

ROS production following ccPDT treatment. In PF-PDT alone with a relatively high fluence rate (35 mW/cm^2) and light dose (6.6 J), ROS production was increased by 33.7±19.9% compared with the untreated control, while ccPDT demonstrated enhanced ROS production by a factor of 2.4 or 1.9 compared with the untreated or PF-PDT alone, respectively (Fig. 4). In PF-PDT alone under irradiation with a relatively lower fluence rate (2.5 mW/cm^2), yields of $OH^{\bullet}$ and $O_2^{\bullet-}$ were residual and did not increase with higher light doses, and were much smaller than those in ccPDT (Fig. 5). However, ROS detection based on ROSstar™ 650 increased with increasing light doses even in the PF-PDT alone treatment group, indicating enhancement of H_2O_2 with increasing light doses in the PF-PDT alone group (Fig. 5C and D). In contrast, ccPDT showed enhanced production of $O_2^{\bullet-}$ by a factor of 3 on average over the range of irradiation doses and a gradual increment of the $OH^{\bullet}$ yield over the range of light doses. In the Type I reaction of PDT, electron transfer to triplet oxygen can produce $O_2^{\bullet-}$. In ccPDT, the residual $O_2^{\bullet-}$ in PDT alone increased sharply, but saturated quickly with increasing light doses. In contrast, the yield of $OH^{\bullet}$ in the combined treatment group was highly enhanced compared to PDT alone, and this enhancement increased with higher light doses, but remained residual in PDT alone. The 50% enhanced production of H_2O_2 by the dismutase-mediated conversion of $O_2^{\bullet-}$ was observed to increase gradually with increasing light doses in the combined treatment group (ccPDT) (Fig. 5D).

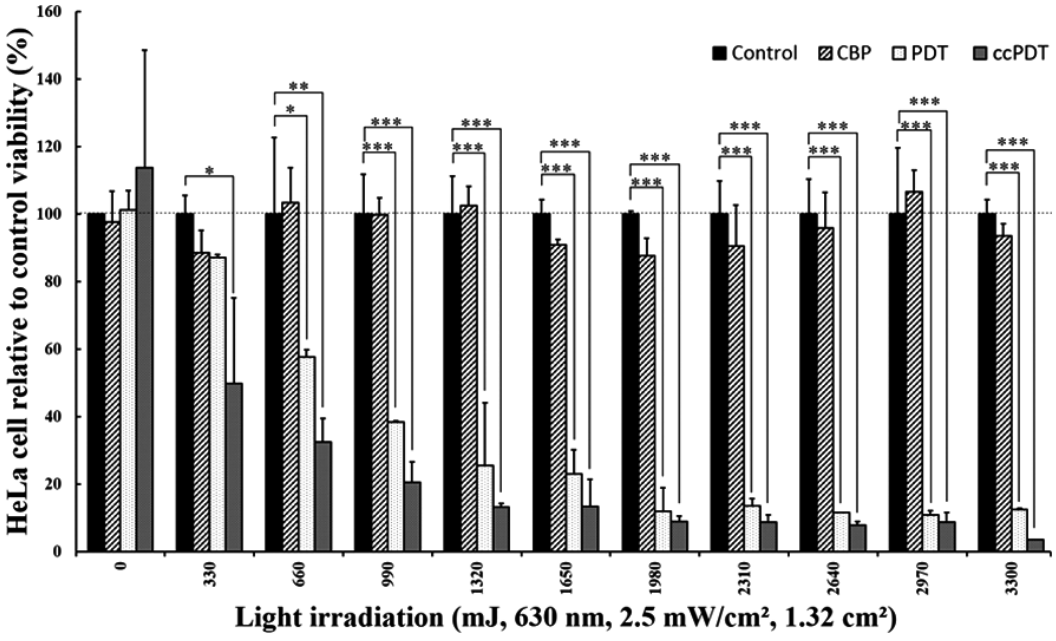

Figure 2. Cytotoxicity of HeLa cells when treated with increasing doses of light irradiation under control (no drug, light only), 20 μM Photofrin only (PF), 100 μM carboplatin only (CBP), and both Photofrin and carboplatin (PF+CBP) conditions. Cytotoxicity was determined by MTT assay. Data represent mean ± SD (n=4 per group). *P<0.05; **P<0.01; ***P<0.001.

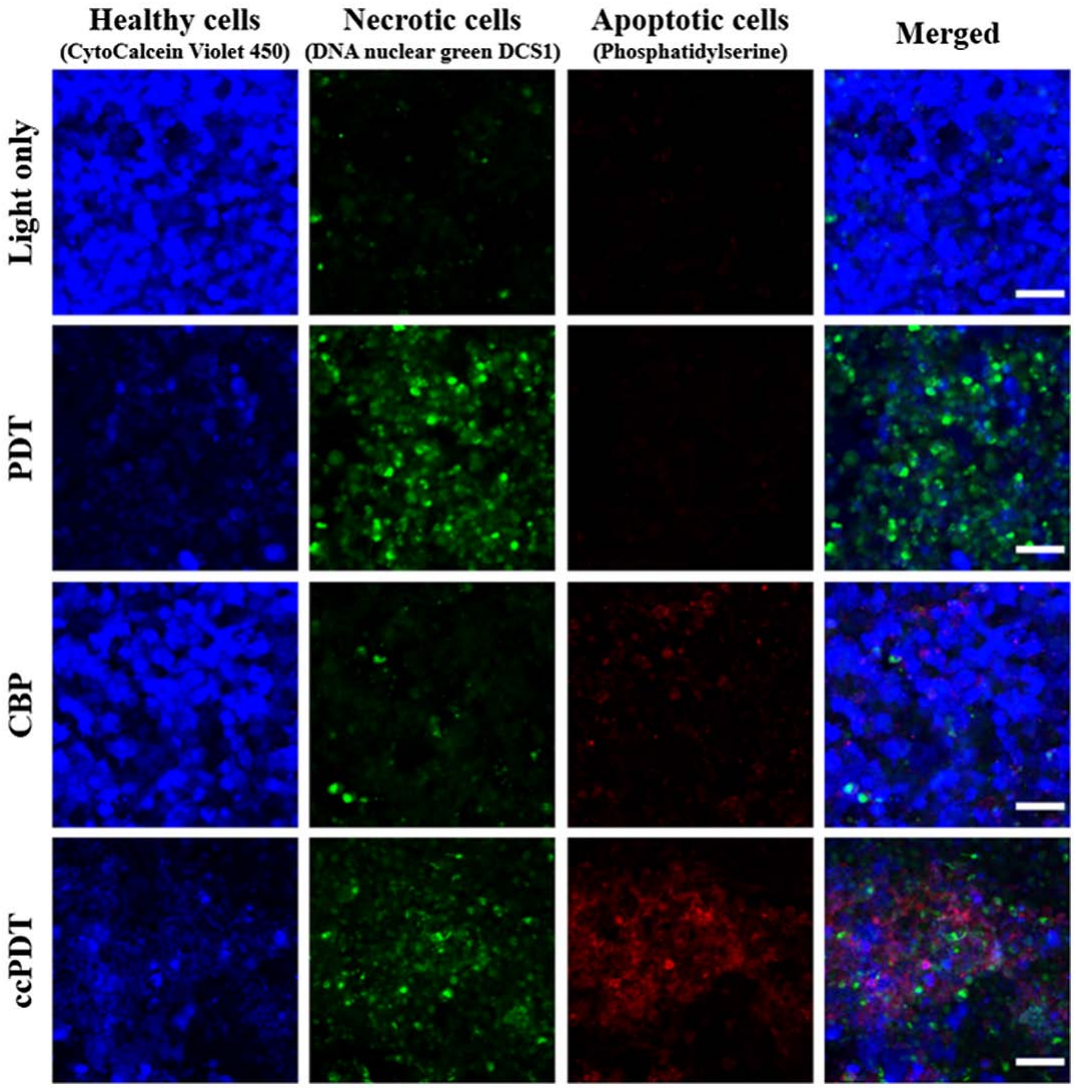

Figure 3. Necrosis and apoptosis assays of HeLa cells treated with light only, 20 μM Photofrin-PDT (PF-PDT), light irradiation in the presence of 100 μM carboplatin only (CBP), and ccPDT. Healthy viable cells were stained with CytoCalcein Violet 450 (blue), necrotic cells with DNA nuclear green DCS1 (green), and apoptotic cells with phosphatidylserine (red). (Nikon A1+, objective: CFI Plan Apo Lambda 10X, NA: 0.45, scale bar: 50 μm). Apoptotic cell death was only 6.0±2.1% following CBP treatment, while 7.3±3.5% cells exhibited necrotic death. In contrast, the apoptotic effect was increased by 35.2±9.4% following ccPDT.

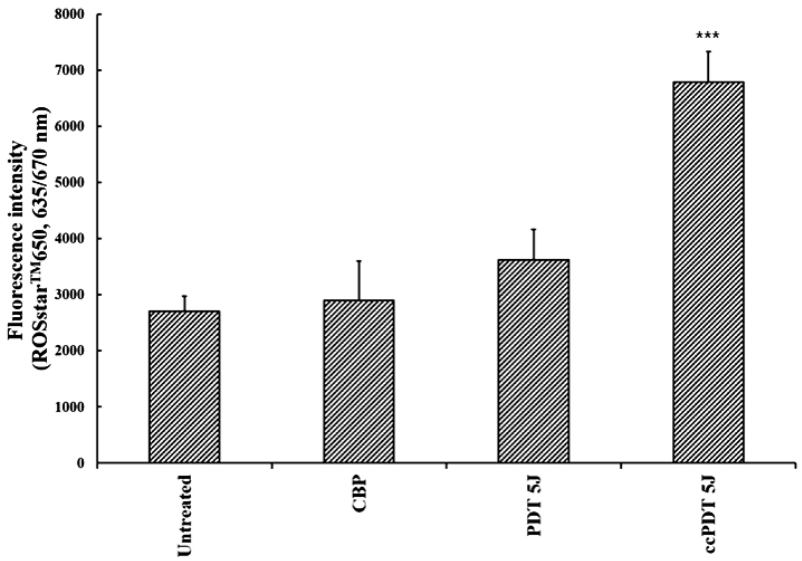

Figure 4. ROS production measured using 10 μM ROSstar™ 650 from the four HeLa cell treatment groups; untreated control, carboplatin only (CBP), PF-PDT (PDT), or ccPDT under 630 nm light irradiation with 35 mW/cm^2 and 5 J. Data represent the mean ± SD (n=4 per group). ***P<0.001.

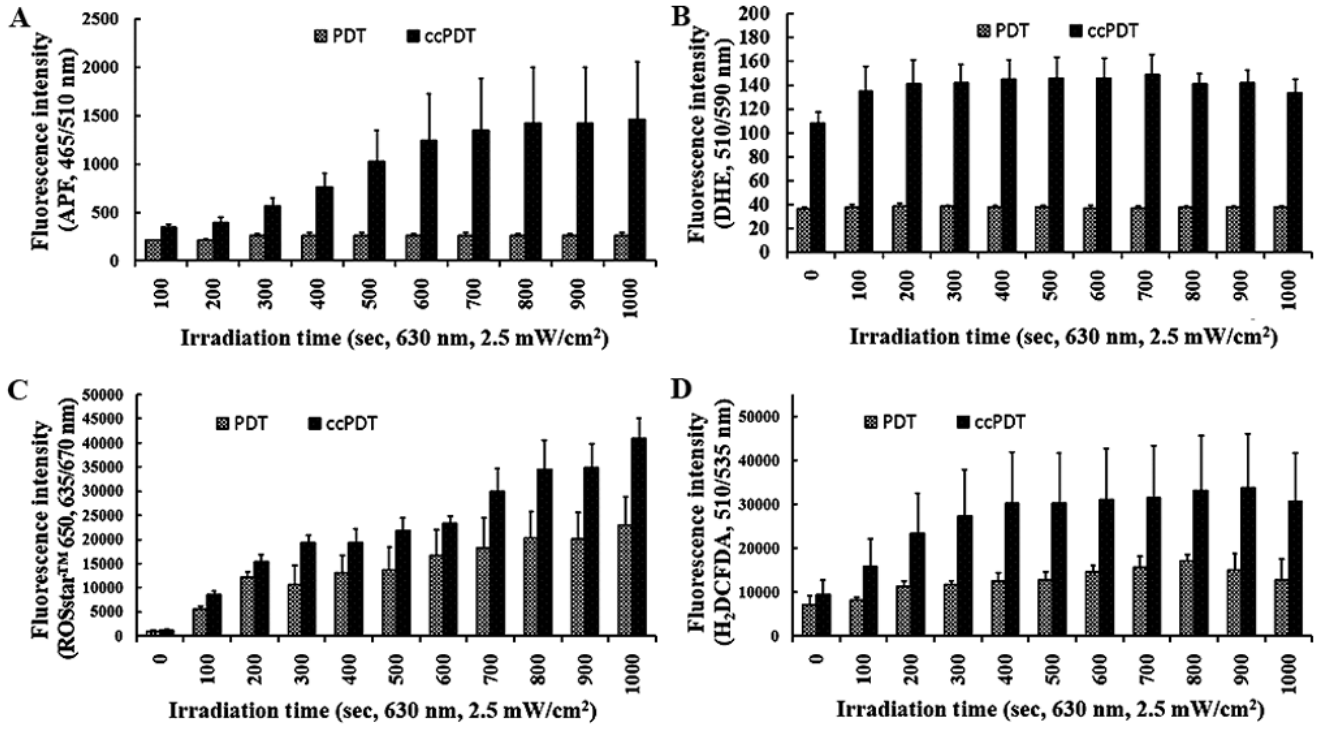

Figure 5. Relative production of (A) hydroxyl radicals, $OH^{\cdot}$ measured by APF, (B) superoxide anions, $O_2^{\cdot-}$ by DHE, (C) $O_2^{\cdot-}$, $OH^{\cdot}$, H_2O_2 by ROSstar™ 650, and (D) intracellular ROS (mainly H_2O_2) by H_2DCFDA between PF-PDT (PDT) and ccPDT with increasing irradiation time. Data represent the mean ± SD (n=5 per group).

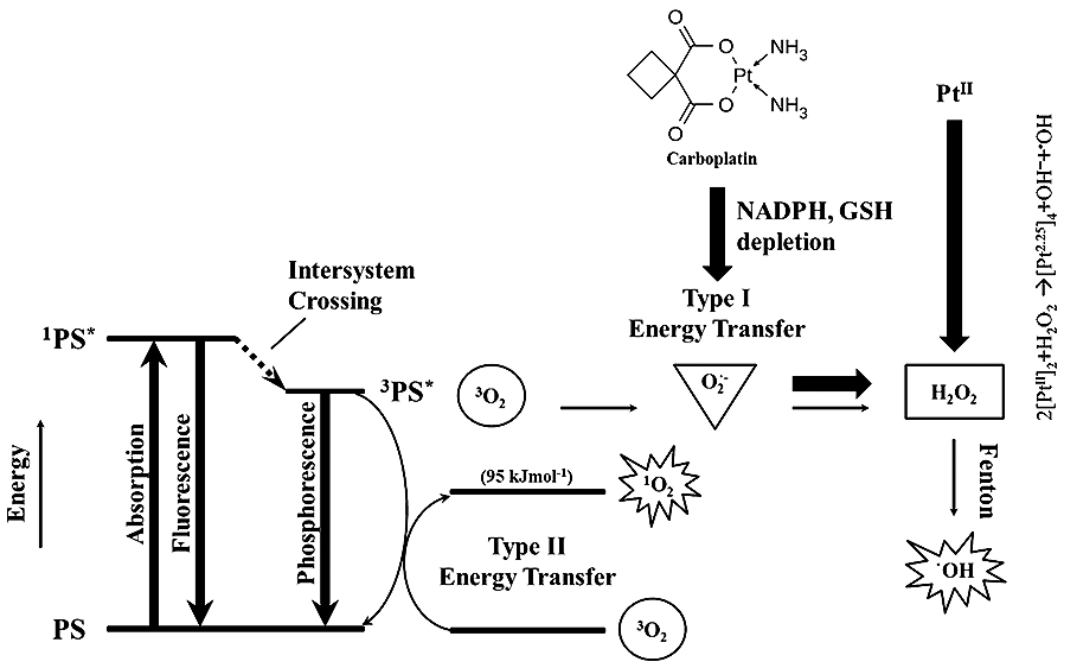

Figure 6. Schematic diagram showing the differential ROS-mediated process between PF-PDT and ccPDT (concurrent low-dose carboplatin Photofrin photodynamic therapy). Carboplatin-mediated enhancement of $O_2^{\cdot-}$ and the Fenton-like reaction are proposed to produce enhanced $OH^{\cdot}$ following ccPDT, whereas $^1O_2$ as the primary damaging species and conversion of $O_2^{\cdot-}$ into $OH^{\cdot}$ via the Fenton reaction on H_2O_2 is limited due to the much lower electron transfer rate compared to the energy transfer following PF-PDT (Photofrin-Photodynamic therapy).

Discussion

Concurrent ccPDT was found to produce hydroxyl radicals as the major additional ROS compared to the prevalent singlet oxygen following PF-PDT alone. The most common oxidation states of platinum are +2 (d^8) and +4 (d^6) (8). Cisplatin and carboplatin are typical Pt^{II} drugs when the preferred oxidation state of the Pt center is +2. CBP-stimulated production of $O_2^{\cdot-}$ can be converted to H_2O_2 by cellular dismutase (14-16), which can be further transformed into $OH^{\cdot}$ by means of either the

CBP-mediated Fenton-like reaction via a light-mediated redox active platinum ion (17-19) or the Fe^{+2}-mediated Fenton reaction from oxidized [4Fe-4S] clusters of proteins (20,21) under the combined regime, as shown in the following equation:

$$2[Pt^{II}]_2 + H_2O_2 \rightarrow [Pt^{2.25}]_4 + OH^- + {}^{\bullet}OH$$

This synergistic reaction may result in enhanced reactive conversion of CBP in the presence of PDT-mediated oxygen radicals under the ccPDT regime (18,19). The notable increase in the $OH^{\bullet}$ yield and relatively constant $O_2^{\bullet-}$ yield with a light dose supports the hypothesis for a Fenton-like reaction via photoactivated CBP. On the other hand, $O_2^{\bullet-}$ contributes to the iron release by oxidizing the [4Fe-4S] clusters (22), which acts as a catalyst for H_2O_2 decomposition in the Fenton reaction, producing more $OH^{\bullet}$ (20,21). In normal untreated cells, H_2O_2 as a metabolic byproduct can then be removed through enzymatic reactions (e.g., catalase) and thiol-systems (e.g. glutathione) to avoid the Fenton reaction formation of $OH^{\bullet}$. In PF-PDT-treated cells, cellular removal of H_2O_2 may be partially impaired as a result of damage to the removal pathway or because the Fenton reaction-mediated conversion to OH^- is limited by a much lower electron transfer rate ($k \leq 1x10^7\ M^{-1}sec^{-1}$) compared to a higher rate of energy transfer ($k \leq 1\text{-}3x10^9\ M^{-1}sec^{-1}$) (23). These results led to the residual accumulation of dose-dependent intracellular H_2O_2 (Fig. 5D), and lipid peroxidation contributing to necrotic damage together with the primary damaging species, $^1O_2$. In the presence of CBP under ccPDT, the Pt^{II} oxidation status enables CBP to easily react with soft bases such as sulfur-containing glutathione (GSH) and other cysteine-rich molecules (8). CBP-stimulated production of $O_2^{\bullet-}$ may lead to the decrease in protective antioxidant systems, and effectively sensitizing the cell to oxidative stress via GSH and NADPH depletion (6,16,24).

The generation of $OH^{\bullet}$ can result in a cascade of different ROS, each with unique properties and preferred biological targets. Necrotic death was a main pathway of cellular damage by Photofrin-mediated PDT under the present regime, as observed in Fig. 3, whereas the apoptotic effects were superimposed in ccPDT as shown also in another report (7). However, in general, the pathway for PF-PDT-mediated cell damage depended on the concentration of PF and the light dose as revealed in previous research (25). In the present study we aimed to demonstrate enhanced production of hydroxyl radicals and related apoptotic effects under only current ccPDT (concurrent low-dose CBP and conventional PF-PDT) regime. General dependency of cellular death on the PF-concentration was not pursued in this study. This enhanced apoptosis can be initiated by the CBP-induced mitochondrial-ROS response (14-16) with depletion of the antioxidant enzyme; however, apoptosis did not occur significantly under CBP alone, as shown in the individual CBP only group (Fig. 3). This result was largely enhanced by accumulated $OH^{\bullet}$ (12,13), suggesting a synergistic effect by ccPDT. A similar effect was reported following cisplatin treatment showing NADPH depletion, which resulted in an altered mitochondrial redox status that then caused the generation of $OH^{\bullet}$ and induction of apoptosis (26-28). Overall, determining the outcome of PDT on a cellular level is complex. Nevertheless, some general themes can be observed (29). With high doses of PDT or PS localization to the plasma membrane, necrosis is the dominant form of cell death. With mild PDT and damage to the mitochondria or anti-apoptotic components, apoptosis is triggered. With low PDT-induced damage to organelles, autophagy is initiated to repair the damage (30). Therefore, in PF-PDT with conventional light dose where PF is localized mainly to the plasma membrane, autophagy may not be the major mechanism of cellular damage in this ccPDT despite application of variable light dose.

ROS-mediated therapeutic efficacy is depicted in Fig. 6. In summary, these results suggest that in Photofrin-PDT alone, necrotic damage is obtained by a $^1O_2$-mediated Type II reaction, while $O_2^{\bullet-}$ is converted into H_2O_2, which is not removed efficiently due to partially impaired antioxidant systems under PDT. Conversely, in ccPDT, production of $O_2^{\bullet-}$ is enhanced by CBP, and H_2O_2 can be further converted into more toxic OH^- via both the potent CBP-mediated Fenton-like reaction and enhancement of the oxidized [4Fe-4S]-mediated Fenton reaction. Therefore, the therapeutic enhancement in low-dose CBP-based ccPDT may be due to the exploitation of the synergistic enhancement of OH^- that led to superimposed apoptosis-based cellular death, while avoiding side effects by reducing the effective dosage of carboplatin.

Acknowledgements

The authors thank Ahn Jin-Cheol of the Medical Laser Research Center, Dankook University for the laser equipment.

Funding

The present study was supported in part by a grant from the Catholic University of Daegu (no. 20175003) and the Industrial Materials Fundamental Technology Development Program (no. 10062194).

Availability of data and materials

The datasets used during the present study are available from the corresponding author upon reasonable request.

Authors' contributions

CYS and CJE performed experiment. CYS and KJK designed the study. JSH reviewed and edited the manuscript. KJK wrote the manuscript. All authors read and approved the manuscript and agree to be accountable for all aspects of the research in ensuring that the accuracy or integrity of any part of the work are appropriately investigated and resolved.

Ethics approval and consent to participate

Not applicable.

Consent for publication

Not applicable.

Competing interests

The authors report no conflicts of interest.

References

1. Ahn TG, Lee BR, Kim JK, Choi BC and Han SJ: Successful full term pregnancy and delivery after concurrent chemo-photodynamic therapy (CCPDT) for the uterine cervical cancer staged 1B1 and 1B2: Preserving 4 fertility in young women. Gynecol Oncol Case Rep 2: 54-57, 2012.
2. Rizvi I, Celli JP, Evans CL, Abu-Yousif AO, Muzikansky A, Pogue BW, Finkelstein D and Hasan T: Synergistic enhancement of carboplatin efficacy with photodynamic therapy in a three-dimensional model for micrometastatic ovarian cancer. Cancer Res 70: 9319-9328, 2010.
3. Biswas R, Mondal A and Ahn JC: Deregulation of EGFR/PI3K and activation of PTEN by photodynamic therapy combined with carboplatin in human anaplastic thyroid cancer cells and xenograft tumors in nude mice. J Photochem Photobiol B 148: 118-127, 2015.
4. Mao W, Sun Y, Zhang H, Cao L, Wang J and He P: A combined modality of carboplatin and photodynamic therapy suppresses epithelial-mesenchymal transition and matrix metalloproteinase-2 (MMP-2)/MMP-9 expression in HEp-2 human laryngeal cancer cells via ROS-mediated inhibition of MEK/ERK signalling pathway. Lasers Med Sci 31: 1697-1705, 2016.
5. Hwang H, Biswas R, Chung PS and Ahn JC: Modulation of EGFR and ROS induced cytochrome c release by combination of photodynamic therapy and carboplatin in human cultured head and neck cancer cells and tumor xenograft in nude mice. J Photochem Photobiol B 128: 70-77, 2013.
6. Peterson K, Harsh G IV, Fisher PG, Adler J and Le Q: Daily Low-dose carboplatin as a radiation sensitizer for newly diagnosed malignant glioma. J Neurooncol 53: 27-32, 2001.
7. He P, Ahn JC, Shin JI, Hwang HJ, Kang JW, Lee SJ and Chung PS: Enhanced apoptotic effect of combined modality of 9-hydroxypheophorbide alpha-mediated photodynamic therapy and carboplatin on AMC-HN-3 human head and neck cancer cells. Oncol Rep 21: 329-334, 2009.
8. Jungwirth U, Kowol CR, Keppler BK, Hartinger CG, Berger W and Heffeter P: Anticancer activity of metal complexes: Involvement of redox processes. Antioxid Redox Signal 15: 1085-1127, 2011.
9. Agostinis P, Berg K, Cengel KA, Foster TH, Girotti AW, Gollnick SO, Hahn SM, Hamblin MR, Juzeniene A, Kessel D, *et al*: Photodynamic therapy of cancer: An update. CA Cancer J Clin 61: 250-281, 2011.
10. Ogilby PR: Singlet oxygen: There is indeed something new under the sun. Chem Soc Rev 39: 3181-3209, 2010.
11. Buytaert E, Dewaele M and Agostinis P: Molecular effectors of multiple cell death pathways initiated by photodynamic therapy. Biochim Biophys Acta 1776: 86-107, 2007.
12. Matroule JY, Carthy CM, Granville DJ, Jolois O, Hunt DW and Piette J: Mechanism of colon cancer cell apoptosis mediated by pyropheophorbide-A methylester photosensitization. Oncogene 20: 4070-4084, 2001.
13. Li D, Li L, Li P, Li Y and Chen X: Apoptosis of HeLa cells induced by a new targeting photosensitizer-based PDT via a mitochondrial pathway and ER stress. Onco Targets The 8: 703-711, 2015.
14. Husain K, Jagannathan R, Hasan Z, Trammell GL, Rybak LP, Hazelrigg SR and Somani SM: Dose response of carboplatin-induced nephrotoxicity in rats. Pharmacol Toxicol 91: 83-89, 2002.
15. Husain K, Whitworth C, Somani SM and Rybak LP: Carboplatin-induced oxidative stress in rat cochlea. Hear Res 159: 14-22, 2001.
16. Kishore Reddy YV, Sreenivasula Reddy P and Shivalingam MR: Cisplatin or carboplatin caused suppression in anti-oxidant enzyme defense system in liver, kidney and testis of male albino rats. J Biomed Sci and Res 2: 23-28, 2010.
17. Bernhard L: Cisplatin: Chemistry and biochemistry of leading anticancer drug. Wiley-VCH; 1st edition, Zurich, Switzerland, pp464, 1999.
18. Tonetti M, Giovine M, Gasparini A, Benatti U and De Flora A: Enhanced formation of reactive species from *cis*-diammine-(1,1-cyclobutanedicarboxylato)-platinum(II) (carboplatin) in the presence of oxygen free radicals. Biochem Pharmacol 46: 1377-1383, 1993.
19. Deavall DG, Martin EA, Horner JM and Roberts R: Drug-induced oxidative stress and toxicity. J Toxicol 2012: 645460, 2012.
20. Kim JH, Bothe JR, Alderson TR and Markley JL: Tangled web of interactions among proteins involved in iron-sulfur cluster assembly as unraveled by NMR, SAXS, chemical crosslinking, and functional studies. Biochim Biophys Acta 1853: 1416-1428, 2015.
21. Tracey Rouault (ed): Iron-Sulfur Clusters in Chemistry and Biology. Walter de Gruyter GmbH & Co KG, p300, 2014.
22. Benov L: How superoxide radical damages the cell. Protoplasma 217: 33-36, 2001.
23. Davies MJ: Reactive species formed on proteins exposed to singlet oxygen. Photochem Photobiol Sci 3: 17-25, 2004.
24. Afanas'ev IB: Superoxide Ion: Chemistry and Biological Implications Vol II Oxygen radicals in Biology. CRC Press, p54, 1991.
25. Gao S, Zhang M, Zhu X, Qu Z, Shan T, Xie X, Wang Y and Feng X: Apoptotic effects of Photofrin-Diomed 630-PDT on SHEEC human esophageal squamous cancer cells. Int J Clin Exp Med 8: 15098-15107, 2015
26. Marullo R, Werner E, Degtyareva N, Moore B, Altaville G, Ramalingam SS and Doetsch PW: Cisplatin induces a mitochondrial-ROS response that contributes to cytotoxicity depending on mitochondrial redox status and bioenergetics fucntions. PLoS One 8: E81162, 2013.
27. Martins NM, Santos NA, Curti C, Bianchi ML and Santos AC: Cisplatin induces mitochondrial oxidative stress with resultant energetic metabolism impairment, membrane rigidification and apoptosis in rat liver. J Appl Toxicol 28: 337-344, 2008.
28. Mandic A, Hansson J, Linder S and Shoshan MC: Cisplatin induces endoplasmic reticulum stress and nucleus-independent apoptotic signaling. J Biol Chem 278: 9100-9106, 2003.
29. Mroz P, Yaroslavsky A, Kharkwal GB and Hamblin MR: Cell death pathways in photodynamic therapy of cancer. Cancers 3: 2516-2539, 2011.
30. van Straten D, Mashayekhi V, de Bruijn HS, Oliveira S and Robinson DJ: Oncologic photodynamic therapy: Basic principles, current clinical status and future Directions. Cancers 9: pii: E19, 2017.